Performance Evaluation of a New Taylor-Flow Grinder in Manufacturing Carboxymethylated Nanofibrillated Cellulose

Ji Hyun Tak,[a] Sung Gyu Park,[a] Ji Young Lee ,[b,*] and Ro Seong Park [c]

Nanofibrillated celluloses (NFCs) are of high economic value owing to their inherent properties, and the deployed manufacturing technology is critical to producing high-quality NFCs. The grinding efficiency determines the quality of mechanically fibrillated NFCs. Previously, a finished Taylor-flow grinder was developed by addressing the operating issues and drawbacks of a prototype grinder and, subsequently, a pilot grinder. This study evaluated the grinding efficiency of the Taylor-flow grinder using hardwood bleached kraft pulp (Hw-BKP) as a raw material, carboxymethylated with monochloroacetic acid and other chemicals. Afterward, two sets of carboxymethylated NFCs (CM-NFCs) were prepared using the finished Taylor-flow grinder and a commercial micro-grinder (commercial grinder) for comparison. To do this, the characteristics of the products obtained using both grinders were determined to evaluate the grinding efficiency of the grinder and that of the representative commercial grinder. The results confirmed that the CM-NFCs prepared with the grinder exhibited higher fiber width and lower viscosity than those prepared using the commercial grinder. Moreover, they were relatively uniform and transparent compared with those prepared with the commercial grinder. Thus, a finished Taylor-flow grinder was developed and demonstrated for manufacturing CM-NFCs with higher qualities from Hardwood kraft pulp.

DOI: 10.15376/biores.20.1.438-451

Keywords: Taylor flow grinder; Commercial micro grinder; Nano-fibrillated cellulose (NFC); Carboxymethylation (CM); Fiber width; Viscosity, Zeta-potential

*Contact information: a: Department of Forest Products, Gyeongsang National University, Jinju 52828, Republic of Korea; b: Department of Environmental Materials Science/IALS, Gyeongsang National University, Jinju 52828, Republic of Korea; c: ESYNDMT, Busan 46977, Republic of Korea; * Corresponding author: paperyjy@gnu.ac.kr*

INTRODUCTION

Nanofibrillated celluloses (NFCs) are materials that have been rendered nano-sized by various mechanical treatments of cellulose fibers into fibers with widths of 1 to 100 nm (Khali *et al*. 2014; Perić *et al*. 2019; Marques *et al*. 2024). As NFCs exhibit high strength and elastic moduli, excellent specific surface area (SSA), dimensional and thermal stabilities, biodegradability, and biocompatibility, many countries, such as the United States, Finland, and Japan, are actively financing the exploration of technologies for manufacturing and utilizing these NFCs or cellulose nanofibrils (CNFs) (Lichtenstein and Lavoine 2017; Mohamad *et al*. 2017; Kono *et al*. 2021; Petroudy *et al*. 2021; Deerattrakul *et al*. 2023; Garcia *et al*. 2024). According to forecasts by major consulting companies, the global CNF market will grow annually by over 20%, growing into a $780 million market

in 2025 (Future Markets, Inc. 2024; Grand View Research 2024). Therefore, efficient NFC-manufacturing and -utilization technologies must be developed.

NFC-manufacturing processes comprise a combination of different operations, which are varied to obtain various types of NFCs. As NFC fibrillation requires intensive mechanical treatments, cellulosic fibers are pretreated before mechanical fibrillation. Notably, several mechanical fibrillation methods (*e.g.*, high-pressure homogenization, microfluidization, grinding, and high-intensity ultrasonication) have been employed to transform cellulosic fibers into nanofibrils (Khali *et al*. 2014; Nechyporchuk *et al*. 2016; Yi *et al*. 2020; Fernades *et al*. 2023). For example, high-pressure homogenizers are fast and effective continuous devices that can obtain laboratory-scale mechanical fibrillation results that are perfectly reproducible on an industrial scale. However, homogenization requires many cycles and consumes high energy (Nair and Yan 2015; Zhang *et al*. 2020; Petroudy *et al*. 2021; Arfelis *et al*. 2023). Conversely, grinding exhibits several advantages over other methods. For example, grinding exhibits high commercial-scale-up potential, as it can be used to fibrillate larger quantities of cellulose fibers than other mechanical methods. Moreover, grinders can fibrillate long fibers without any pretreatment and circumvent the clogging issue associated with mechanical fibrillation (Siro and Plackett 2010; Nair and Yan 2015). Nevertheless, as grinding also requires numerous cycles to obtain uniform nanofibrils, developing a new grinding device for manufacturing NFCs more effectively by circumventing the numerous-cycle issue is necessary.

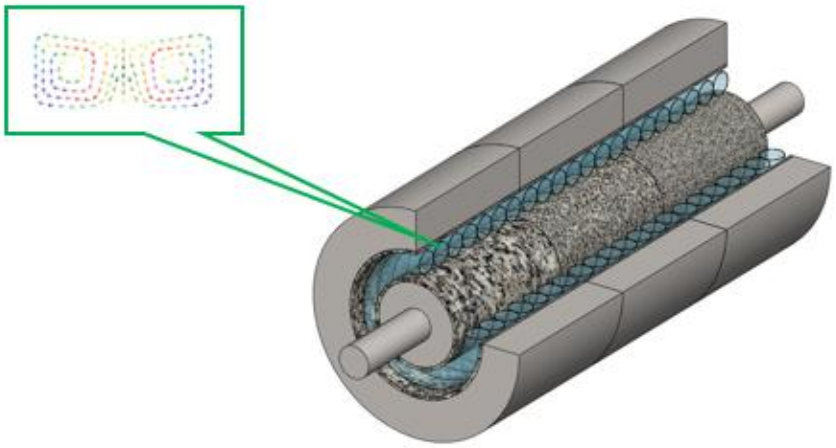

Fig. 1. Grinding cylinder of a Taylor flow grinder developed in this study

A commercial micro-grinder (commercial grinder hereinafter) fibrillates cellulosic fibers by a shearing force generated at the edge where two grinding stones meet. Its efficiency can be improved by increasing the exposure time of the cellulose fibers to the applied shear force when they pass through the grinder (Lahtinen *et al*. 2014; Petroudy *et al*. 2021; Uranchimeg *et al*. 2022). However, as the two stones meet at a linear point rather than plane one, there is a limit to which the fibrillation time can be increased. Moreover, a long fibrillation time corresponds to a high grinding efficiency for manufacturing NFCs from cellulose fibers.

Previously, a Taylor-flow grinder was developed for NFC production (Lee *et al*. 2021; Jo *et al*. 2022a,b; 2023). Taylor-flow arises when viscous fluid is confined in the gap between rotating cylinders. This type of device has become a reference in hydrodynamic

stability studies due to the gradual destabilizing of a flow, lending itself to a rigorous mathematical approach (Fenot *et al*. 2011). It has been found that steady laminar motion is possible if the motion is sufficiently slow, but that if the velocity of the fluid exceeds a certain limit, depending on the viscosity of the fluid and the configuration of the boundaries, the steady motion breaks down and eddying flow sets in (Taylor 1923). This new grinder, based on the Taylor flow of a pulp slurry, follows a different fiber-fibrillation mechanism compared with the commercial grinder. The Taylor or Taylor–Couette flow is the viscous fluid flow when confined in the gap between two rotating cylinders; a round bar-type cylinder is inserted into a pipe-type one (Davey 1962; Xu *et al*. 2021). Figure 1 shows a schematic of the grinding cylinder of a Taylor-flow grinder. The grinder cylinder was designed to induce the uniform and efficient fibrillation of a pulp suspension through Taylor flow by extending the fibrillation and retention time of the pulp slurry in the grinding cylinder. Detailed information on Taylor-flow grinders will be described in the Experimental section.

Various versions of the grinders have been manufactured, and their performances have been evaluated by comparing the characteristics of the obtained NFCs (Lee *et al*. 2021; Jo *et al*. 2022a,b; 2023). Finally, a finished Taylor-flow grinder was developed by compensating the drawbacks of a prototype Taylor-flow grinder and a pilot one. In this study, a finished Taylor flow grinder was manufactured, and two sets of carboxymethylated NFCs (CM-NFCs) were prepared from bleached hardwood kraft pulp (Hw-BKP) using the finished Taylor-flow grinder and the commercial grinder (as a control). After that, the characteristics of both sets of CM-NFCs were analyzed to evaluate the grinding efficiency of the finished Taylor-flow grinder.

EXPERIMENTAL

Materials

The raw material (Hw-BKP) was supplied by Moorim Paper Co., Ltd. (Jinju, Republic of Korea). Table 1 presents information about the chemicals used for the carboxymethylation of Hw-BKP, as well as the measurement of the fiber width of the NFC.

Table 1. Chemicals for Hw-BKP Carboxymethylation and the Measurement of the Fiber Width of CM-NFCs

Chemical	Molecular formula	Concentration	Manufacturer
Monochloroacetic acid (MCA)	$ClCH_2COOH$	99.0%	Yakuri Pure Chemicals
Sodium hydroxide	NaOH	98.0%	Samchun
Sodium hydrogen carbonate	$NaOCO_3$	99.8%	Yakuri Pure Chemicals
Isopropanol	$CH_3CHOHCH_3$	99.5%	Duksan Reagents
Ethanol	CH_3CH_2OH	99.9%	Duksan Reagents
Methanol	CH_3OH	99.9%	Fisher Scientific
n-Hexane	$CH_3(CH_2)_4CH_3$	99.9%	Fisher Scientific

Methods

Development process of the Taylor flow grinder

Figure 2 shows three Taylor-flow-grinder versions, and Table 2 presents the specifications of their grinding cylinders. A Taylor-flow grinder generally comprises a

grinding cylinder (grinder), a mixer, a pump, and a cooler. The grinding cylinder comprises a rotor and a stator to induce Taylor-flow-driven uniform dispersion and fibrillation and increase the grinding time. The rotor and stator comprised three stages to allow for the electrodeposition of diamond particles on their surfaces based on the characteristics of the grinding materials. The stirrer was designed to control the capacity and stirring speed to ensure the uniform dispersion of the pulp slurry as well as its delivery to the grinding cylinder through the pump. Amount of heat is generated during grinding; a cooler is installed to lower the temperature of the grinding cylinder because a high temperature hinders the fibrillation of cellulose fibers in the grinding cylinder.

The finished Taylor-flow grinder was fabricated by complementing the drawbacks of the previously developed prototype and, subsequently, the pilot grinder. Compared with the pilot and finished grinder, the inner diameters of the rotor and stator in the finished grinder were enlarged from 120 to 240 mm, and the gap was adjusted from 0.14 to 0.11 mm. Additionally, the size of the electrodeposited diamond particles on the rotor and stator surfaces decreased from 80 to 100 mesh. Figure 3 shows the detailed structure of the finished grinder cylinder. The capacity of the finished grinder was increased to 9,600 mL/h, and a cooling device of an appropriate capacity was supplemented to control the high-heat generation of the grinding cylinder. A multistage centrifugal pump was applied to the metering pump to facilitate the high-pressure transport of the pulp slurry (a discharge pressure of up to 0.7 MPa was realized).

Table 2. Grinding Cylinders' Specifications of Three Versions of Taylor Flow Grinders

Specifications of grinding cylinder	Prototype	Pilot	Finished
Diameter of stator and rotator (mm)	60	120	240
The gap between the rotator and stator (mm)	0.14	0.14	0.11
Grinding cylinder capacity (mL/h)	600	2,400	9,600
Size of the diamond particle (mesh)	80	80	100

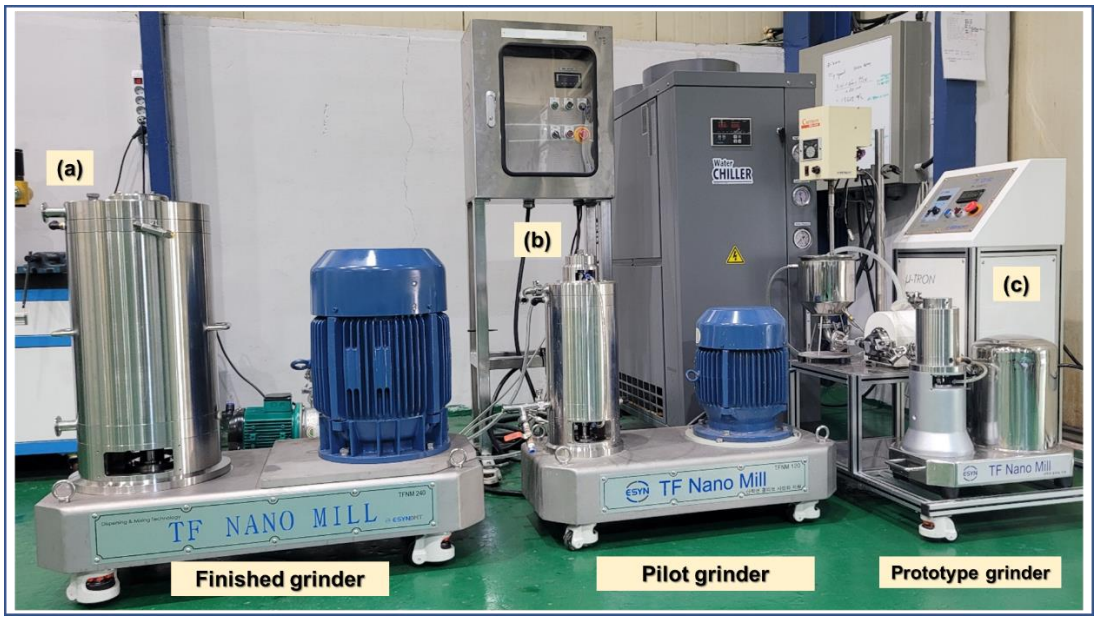

Fig. 2. Pictures of the prototype, pilot, and finished Taylor-flow grinders

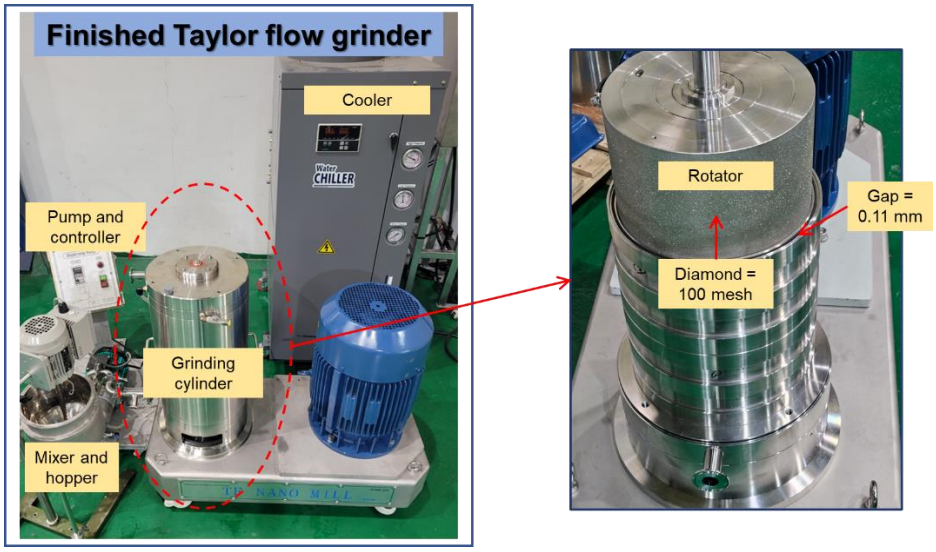

Fig. 3. Pictures of the finished Taylor flow grinder (Permission granted from Korea Technical Association of The Pulp and Paper Industry; Jo *et al*. 2023)

Carboxymethylation of bleached hardwood kraft pulp (Hw-BKP)

Hw-BKP (solid content: 1.57% solid) was soaked in tap water and beaten to Canadian Standard Freeness (CSF, 450 ± 5 mL) using a laboratory Hollander beater. The beaten Hw-BKP fibers were dehydrated using a vacuum-filtration system so that the water content was 70%. After that, solvent exchange was performed three times using 500 mL ethanol in each case. Next, the Hw-BKP fibers were added into a mixed solution of NaOH, methanol (150 mL), and isopropanol (600 mL) for 30 min. The carboxymethylation reaction was initiated by adding MCA with continuous stirring at 65 °C for 1 h (Table 3). After the reaction, the Hw-BKP slurry was neutralized with 0.1 M of acetic acid to pH 7 and subsequently washed with distilled water and filtered on a Büchner funnel. The filtered Hw-BKP fibers were immersed in 4% sodium hydrogen carbonate for 1 h to form the Na-form. Afterward, the Hw-BKP slurry was washed with distilled water and filtered with the Büchner funnel to dilute the Hw-BKP slurry to 1% consistency for grinding.

Table 3. Dosage of Chemicals Employed for Hw-BKP Carboxymethylation

Degree of substitution	0.02	0.30
Dosage of NaOH (% on o.d. fibers)	16	100
Dosage of MCA (% on o.d. fibers)	10	100

Preparation of the carboxymethylated nanofibrillated celluloses using the finished Taylor-flow grinder and commercial grinder

The carboxymethylated Hw-BKP (1.0% consistency) was used to prepare CM-NFCs with the finished Taylor-flow grinder and a commercial grinder for comparison. The commercial grinder was used as a control device to compare the main properties of prepared CM-NFCs.

The finished Taylor-flow grinder comprised a grinding cylinder, a mixer, a pump with flow-rate control, a flow meter, a cooler, and a double-jacketed storage tank (Fig. 4).

The grinder cylinder consisted of a rotor and a stator, and their surfaces were made of diamond particles. The carboxymethylated Hw-BKP slurry was added to the mixer and delivered to the grinding cylinder by a pump. The gap between the stator and rotator in the grinder cylinder was adjusted to 0.11 mm, and the speed of the rotator was set to 1900 rpm. After that, the ground Hw-BKP slurry was returned to the mixer and recirculated in the grinder system for a period (Table 4 presents the detailed operating conditions).

Conversely, Super Mass Colloider (MKZA6-2, Masuko Sangyo Co., Ltd., Kawaguchi, Japan) was used as the commercial grinder to prepare CM-NFCs from the same Hw-BKP slurry. Briefly, the pulp slurry was fed continuously to the grinder comprising two stone grinding disks positioned on top of each other at 1,500 rpm (Fig. 5). The gap between the two disks was adjusted to −150 μm. Note that the negative value of the gap is not intended to be taken literally; rather it is inherent in the way that the device presents its report to the user. As the operating principles of the Taylor-flow grinder and commercial grinder differed, the NFC samples were collected at the same grinding time (2, 3, and 4 h) and MCA dosage.

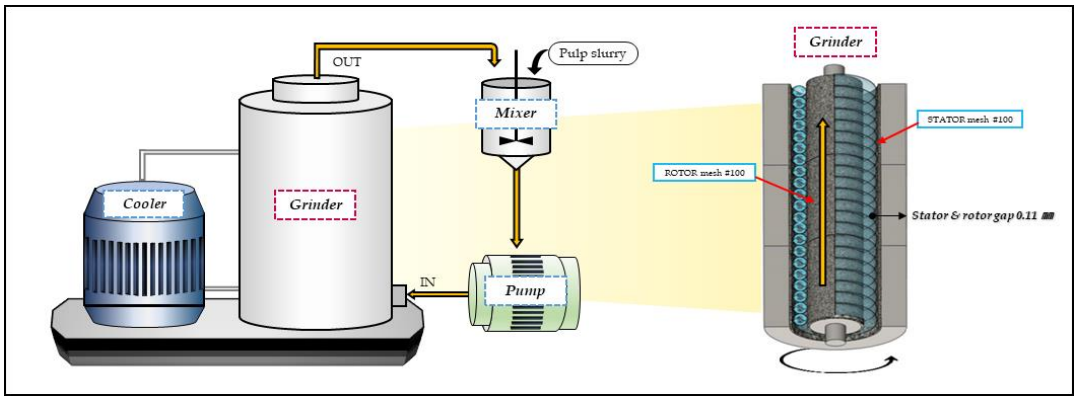

Fig. 4. Schematic of the Taylor flow grinder (Permission granted from Korea Technical Association of The Pulp and Paper Industry; Jo *et al*. 2023)

Table 4. Operating Condition of the Finished Taylor Flow Grinder for Preparing CM-NFCs

Items	Operating Condition
Rotator speed (rpm)	1,900
The gap between the rotator and stator (mm)	0.11
Linear velocity (m/s)	23.864
Grinding time (h)	2, 3, 4

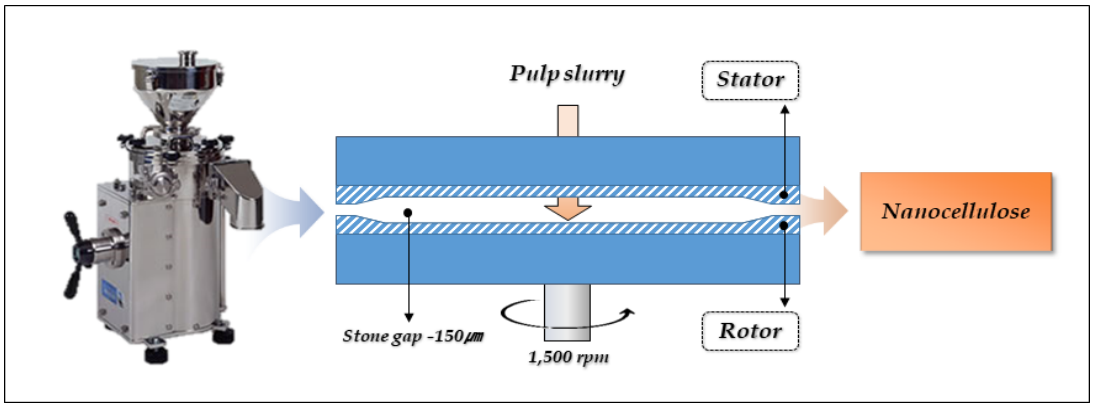

Fig. 5. Operating principle of a commercial grinder

Characterization of the carboxymethylated nanofibrillated cellulose

The fiber width and low-shear viscosity of the NFCs were measured to evaluate their characteristics based on the grinder type, the fibrillation time, and the MCA dosage. The fiber width of the NFCs was analyzed by field-emission scanning electron microscopy (FE-SEM; JSM-7610F, JEOL, Tokyo, Japan). Thus, wet NFC pads were prepared as test specimens to measure the fiber width using a vacuum-filtration system. These wet NFC pads were dried by solvent exchange using ethyl alcohol and n-hexane to provide the dry test specimens (Oh *et al*. 2022). Afterward, the FE-SEM images of the pads were captured, and the fiber width was measured by image analysis using a three-dimensional image software (MP-45030TDI, JEOL, Osaka, Japan). The low-shear viscosity of the 1.0% NFC slurries was determined using a low-shear viscometer (DV-IP, Brookfield Engineering Laboratories, Inc., Middleborough, MA, USA) with a spindle number of 64 and a speed of 60 rpm. The temperature of the NFC slurries was maintained at 25 °C during the viscosity measurement.

To identify the electrostatic properties of the CM-NFCs, the average zeta potential and zeta potential distribution of the 0.01% NFC slurries were measured using a zeta potential analyzer (Nano ZS, Malvern Panalytical, Malvern, UK).

RESULTS AND DISCUSSION

Characteristics of the Prepared Carboxymethylated Nanofibrillated Celluloses

Figures 6 and 7 show the fiber widths of CM-NFCs prepared by the Taylor-flow grinder and the commercial grinder. It was observed that increasing the grinding time and MCA dosage reduced the nanofiber width of the CM-NFCs regardless of the deployed grinder type. When grinding was implemented for 2 to 4 h using the Taylor-flow grinder, the average nanofiber width decreased from 58.4 nm (standard deviation [SD]: 8.7) to 48.1 nm (SD: 6.3) at an MCA dosage of 10%, and the average nanofiber width decreased from 50.1 nm (SD: 5.6) to 38.2 nm (SD: 5.1) at an MCA dosage of 100%. When grinding proceeded from 2 to 4 h using the commercial grinder, the average nanofiber width decreased from 50.4 nm (SD:11.8) to 38.9 nm (SD: 6.4) at an MCA dosage of 10%, and the average fiber width decreased from 42.5 nm (SD: 9.1) to 33.6 nm (SD: 6.0) when the MCA dosage was 100%.

Figures 8 and 9 show the low-shear viscosities of the CM-NFCs prepared using the Taylor-flow grinder and the commercial grinder, respectively. At a grinding time of 2 to 4 h using the Taylor-flow grinder, the viscosity increased from 58.4 to 663.9 cPs at an MCA dose of 10%; the viscosity increased from 2,100 to 2,190 cPs at an MCA dosage of 100%. When grinding proceeded for 2 to 4 h using the commercial grinder, the viscosity increased from 1,869 to 2,817 cPs at an MCA dosage of 10%, increasing from 2,350 to 3,090 cPs at an MCA dosage of 100%.

As the carboxymethylation reaction progressed, the electrostatic properties of NFCs, which are anionic, increased (they became more anionic) with the introduction of carboxymethyl groups to the NFC surface (Li *et al*. 2017; Kono *et al*. 2021; Aguado *et al*. 2023). Figures 10 and 11 show grinding-time- and MCA-dosage-dependent zeta potentials of the CM-NCFs prepared with the Taylor-flow grinder and the commercial grinder, respectively, revealing that the zeta potentials of the CM-NFCs increased in their negative values regardless of the grinder type. In detail, at a grinding time of 2 to 4 h using the Taylor-flow grinder, the average zeta potential decreased from −19.5 mV (SD: 1.1) to −22.2 mV (SD: 0.8) at an MCA dosage of 10% further decreasing from −29.3 mV (SD: 0.9) to −31.9 mV (SD: 0.5) at an MCA dosage of 100%. At the same grinding time using the commercial grinder, the average zeta potential decreased from −26.0 mV (SD: 1.8) to −27.8 mV (SD: 1.8) at an MCA dosage of 10%, further decreasing from −33.0 mV (SD: 1.4) to −34.8 nm (SD: 1.5) at an MCA dosage of 100%. The commercial-grinder-prepared CM-CNFs exhibited higher anionic properties than their Taylor-flow-grinder-prepared counterparts at the same grinding time and MCA dosage because the SSA of CM-CNFs increased with the production of relatively smaller nanofibrils, which further increased the anionic properties of the samples (Grüneberger *et al*. 2014; Rahman *et al*. 2021).

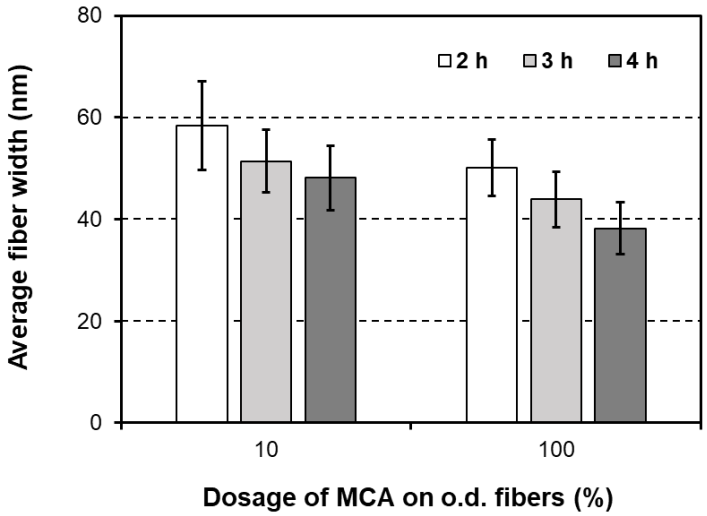

Fig. 6. Average fiber width of the CM-NFCs prepared using the Taylor-flow grinder from the perspectives of the grinding time and MCA dosage

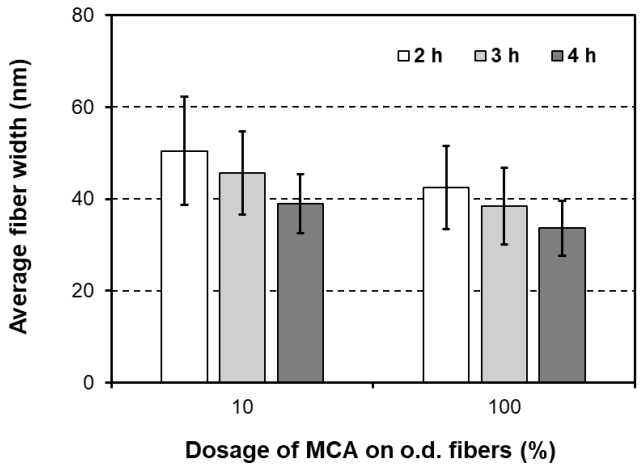

Fig. 7. Average fiber width of the CM-NFCs prepared using the commercial grinder from the perspectives of the grinding time and MCA dosage

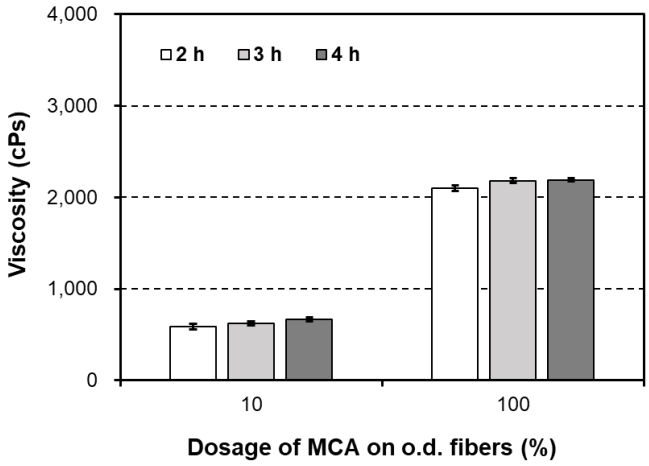

Fig. 8. Low-shear viscosity of the CM-NFCs prepared using the Taylor-flow grinder from the perspectives of the grinding time and MCA dosage

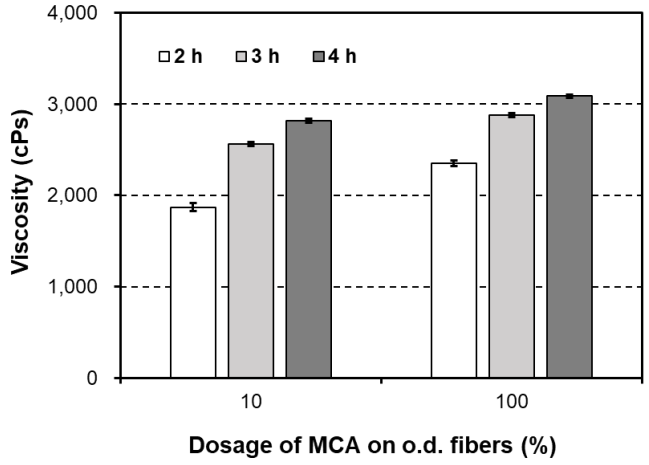

Fig. 9. Low-shear viscosity of the CM-NFCs prepared by the commercial grinder from the perspectives of the grinding time and MCA dosage

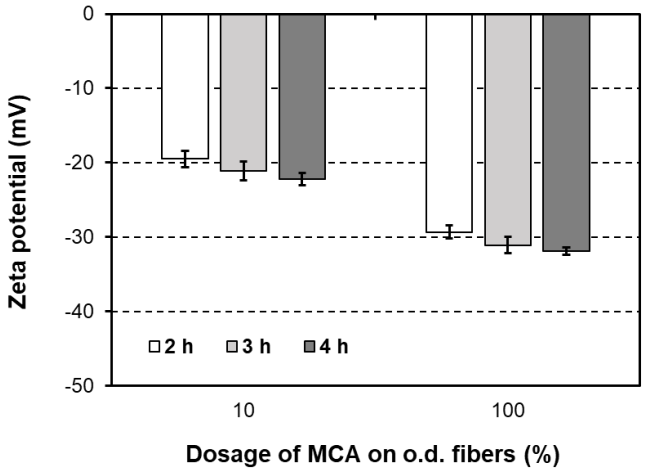

Fig. 10. Average zeta potential of the CM-NFCs prepared using the Taylor-flow grinder from the perspectives of the grinding time and MCA dosage

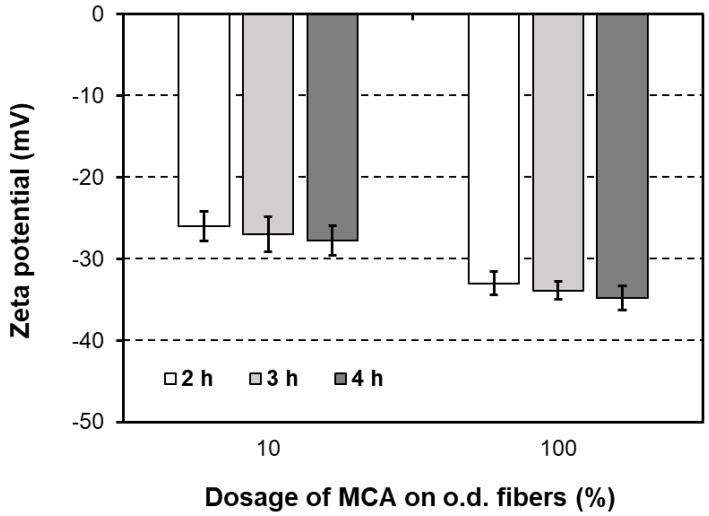

Fig. 11. Average zeta potential of the CM-NFCs prepared using the commercial grinder from the perspectives of the grinding time and MCA dosage

Figure 12 shows the picture of a ground CM-NFC suspension using the finished Taylor-flow grinder for 4 h at a 100% MCA dosage. The photo shows that the CM-NFC suspension was very transparent, indicating that it contained only nanofibrils.

The finished Taylor-flow-grinder-prepared CM-NFCs also exhibited higher fiber width, lower viscosity, and less anionic zeta potential than their commercial-grinder-prepared suspension. However, the finished Taylor-flow grinder manufactured a uniform suspension based on the fiber width and zeta potential results, as well as transparent CM-NFCs. Therefore, the finished Taylor-flow grinder manufactured nano-level fibrils and could be deployed to produce relatively uniform CM-NFCs from Hw-BKPs.

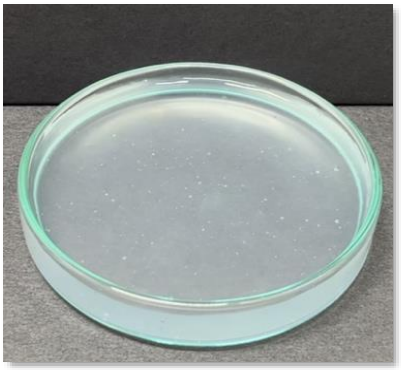

Fig. 12. CM-NFC prepared using the finished Taylor-flow grinder at an MCA dosage of 100%

CONCLUSIONS

1. A finished Taylor-flow grinder comprising a grinding cylinder, mixer, pump with flow-rate control, flow meter, and cooler was produced from an already developed prototype (subsequently pilot grinder) by addressing their operating issues and drawbacks. It exploits Taylor flow to induce uniform flow and increases the pulp-suspension retention time in the grinding cylinder.
2. The Taylor-flow-grinder-prepared carboxymethylated nanofibrillated cellulose (CM-NFC) exhibited higher fiber width, and lower viscosity than their commercial-grinder-prepared counterparts. However, the finished Taylor-flow grinder manufactured relatively uniform nanofibrils, as confirmed by their fiber width and zeta potential, as well as the transparency of the suspension.
3. The finished Taylor-flow grinder manufactured nanofibrils from hardwood bleached kraft pulp (Hw-BKP) and could produce relatively more uniform CM-NFCs than the commercial grinder.

ACKNOWLEDGMENTS

This work was supported by the Collabo R&D between Industry and Academy (S3104789) funded by the Ministry of SMEs and Startups (MSS, Korea).

REFERENCES CITED

Aguado, R. J., Mazega, A., Tarres, Q., and Delgado-Aguilar, M. (2023). "The role of electrostatic interactions of anionic and cationic cellulose derivatives for industrial applications: A critical review," *Industrial Crops and Products* 201, article 116898. DOI: 10.1016/j.indcrop.2023.116898

Arfelis, S., Aguado, R. J., Civancik, D., Fullana-i-Palmer, P., Pelach, M. A., Tarres, Q., and Delgado-Aguilar, M. (2023). "Sustainability of cellulose micro-/nanofibers: A comparative life cycle assessment of pathway technologies," *Science of the Total*

Environment 874, article 162482. DOI: 10.1016/j.scitotenv.2023.162482

Davey, A. (1962). "The growth of Taylor vortices in flow between rotating cylinders," *Journal of Fluid Mechanics* 14(3), 336-368. DOI: 10.1017/S0022112062001287

Deerattrakul, V., Sakulaue, P., Bunpheng, A., Kraithong, W., Pengsawang, A., Chakthranont, P., Iamprasertkun, P., and Itthibenchapong, V. (2023). "Introducing hydrophilic cellulose nanofiber as a bio-separator for 'water-in-salt' based energy storage devices," *Electrochimica Acta* 453, article 142355. DOI: 10.1016/j.electacta.2023.142355

Fénot, M., Bertin, Y., Dorignac, E., and Lalizel, G. (2011). "A review of heat transfer between concentric rotating cylinders with or without axial flow," *Int. J. Therm. Sci.* 50(7), 1138-1155.

Fernades, A., Cruz-Lopes, L., Esteves, B., and Evtuguin, D. (2023). "Nanotechnology applied to cellulosic materials," *Materials* 16(8), article 3104. DOI: 10.3390/ma16083104

Future Markets, Inc. (2024). *The Global Market for Micro- and Nanocellulose 2024-2035*. Future Markets, Inc., New York, NY, USA.

Garcia, K. R., Beck, R. C. R., Brandalise, R. N., and Santos, V. (2024). "Nanocellulose, the green biopolymer trending in pharmaceuticals: A patient review," *Phamaceutics* 16(1), article 145. DOI: 10.3390/pharmaceutics16010145

Grand View Research. (2024). *Nanocellulose Market Size, Share & Trends Analysis Report by Type (Cellulose Nanofibers, Bacterial Cellulose, Crystalline Nanocellulose), by Application, by Region, and Segment Forecasts, 2023 – 2030*, Grand View Research, San Francisco, CA, USA.

Grüneberger, F., Künniger, T., Zimmermann, T., and Martin, A. (2014). "Rheology of nanofibrillated cellulose/acrylate systems for coating applications," *Cellulose* 21, 1313-1326. DOI: 10.1007/s10570-014-0248-9

Jo, H. M., Kim, D. H., Lee, S. H., Lee, J. Y., and Park, N. S. (2022a). "Development of domestic Taylor-flow nanogrinder for manufacturing cellulose nanofiber I - Evaluation of the physical properties of enzyme-pretreated cellulose nanofiber for the performance evaluation of a pilot scale Taylor-flow nanogrinder," *Journal of Korea TAPPI* 54(5), 5-13. DOI: 10.7584/JKTAPPI.2022.10.54.5.5

Jo, H. M., Lee, S. H., Lee, J. Y., and Park, N. S. (2022b). "Development of domestic Taylor-flow nanogrinder for manufacturing cellulose nanofiber II - Evaluation of physical properties of carboxymethylated cellulose nanofibers made from bleached kraft pulps," *J. Korea TAPPI* 54(6), 34-42. DOI: 10.7584/JKTAPPI.2022.12.54.6.34

Jo, H. M., Lee, S. H., Lee, J. Y., and Park, N. S. (2023). "Development of domestic Taylor-flow nanogrinder for manufacturing cellulose nanofiber III - Evaluation of physical properties of cellulose nanofibers manufactured with scale-up Taylor-flow nanogrinder," *J. Korea TAPPI* 55(5), 96-105. DOI: 10.7584/JKTAPPI.2023.10.55.5.96

Khali, H. P. S. A., Davoudpour, Y., Islam, M. N., Mustapha, A., Sudesh, K., Dungani, R., and Jawaid, M. (2014). "Production and modification of nanofibrillated cellulose using various mechanical processes: A review," *Carbohydrate Polymers* 99, 649-665. DOI: 10.1016/j.carbpol.2013.08.069

Kono, H., Tsukamoto, E., and Tajima, K. (2021). "Facile post-carboxymethylation of cellulose nanofiber surfaces for enhanced water dispersibility," *ACS Omega* 6(49), 34107-34114. DOI: 10.1021/acsomega.1c05603

Lahtinen, P., Liukkonen, S., Pere, J., Sneck, A., and Kangas, H. (2014). "A comparative study of fibrillated fibers from different mechanical and chemical pulps," *BioResources* 9(2), 2115-2127. DOI: 10.15376/biores.9.2.2115-2127

Lee, Y. H., Lee, J. Y., Jo, H. M., and Park, N. S. (2021). "Quality evaluation of cellulose nanofiber manufactured with a prototype grinder for the development of a Taylor-flow nanogrinding system," *Journal of Korea TAPPI* 53(4), 98-105. DOI: 10.7584/JKTAPPI.2021.08.53.4.98

Li, Z., Wang, Y., Pei, Y., Xiong, W., Xu, W., Li, B., and Li, J. (2017). "Effect of substitution degree on carboxymethylcellulose interaction with lysozyme," *Food Hydrocolloids* 62, 222-229. DOI: 10.1016/j.foodhyd.2016.07.020

Lichtenstein, K., and Lavoine, N. (2017). "Toward a deeper understanding of the thermal degradation mechanism of nanocellulose," *Polymer Degradation and Stability* 146, 53-60. DOI: 10.1016/j.polymdegradstab.2017.09.018

Marques, A. P. S., Almeida, R. O., Pereira, L. F. R., Carvalho, M. G. V. S., and Gamelas, J. A. F. (2024). "Nanocellulose and their applications in conversation and restoration of historical documents," *Polym.* 16(9), article 1227. DOI: 10.3390/polym16091227

Mohamad, A. M., Mutalib, M. A., Hir, Z. A. M., Zain, M. F. M., Mohamad, A. B., Minggu, L. J., Awang, N. A., and Salleh, W. N. W. (2017). "An overview on cellulose-based material in tailoring bio-hybrid nanostructured photocatalysts for water treatment and renewable energy applications," *International Journal of Biological Macromolecules* 103, 1232-1256. DOI: 10.1016/j.ijbiomac.2017.05.181

Nair, S. S., and Yan, N. (2015). "Bark derived submicron-sized and nano-sized cellulose fibers: From industrial waste to high performance materials," *Carbohydrate Polymers* 134, 258-266. DOI: 10.1016/j.carbpol.2015.07.080

Nechyporchuk, O., Belgacem, M. N., and Bras, J. (2016). "Production of cellulose nanofibrils: A review of recent advances," *Industrial Crops and Products* 93, 2-25. DOI: 10.1016/j.indcrop.2016.02.016

Oh, Y. J., Park, S. Y., Yook, S. Y., Shin, H. N., Lee, H. L., and Youn, H. J. (2022). "A waterproof cellulose nanofibril sheet prepared by the deposition of an alkyl ketene dimer on a controlled porous structure," *Cellulose* 29, 6645-6657. DOI: 10.1007/s10570-022-04701-8

Perić, M., Putz, R., and Paulik, C. (2019). "Influence of nanofibrillated cellulose on the mechanical and thermal properties of poly(latic acid)," *European Polymer Journal* 114, 426-433. DOI: 10.1016/j.eurpolymj.2019.03.014

Petroudy, S. R. D., Chabot, B., Loranger, E., Naebe, M., Shojaeiarani, J., Gharehkhani, S., Ahvazi, B., Hu. J., and Thomas. S. (2021). "Recent advances in cellulose nanofibers preparation through energy-efficient approaches: A review," *Energies* 14(20), article 6792. DOI: 10.3390/en14206792

Rahman, S., Hasan, S., Nitai, A. S., Namn S., Karmakar, A. K., Ahsan, S., Shiddiky, M. J. A., and Ahmed, M. B. (2021). "Recent developments of carboxymethyl cellulose," *Polymers* 13(8), article 1345. DOI: 10.3390/polym13081345

Siro, L., and Plackett, D. (2010). "Microfibrillated cellulose and new nanocomposite materials: A review," *Cellulose* 17(3), 459-494. DOI: 10.1007/s10570-010-9405-y

Taylor, G. I. (1923). "Stability of viscous liquid contained between two rotating cylinders," *Philosophical Transactions of the Royal Society of London Series A* 223

Uranchimeg, K., Jargalsaikhan, B., Bor, A., Yoon, K. Y., and Choi, H. K. (2022). "Comparative study of the morphology of cellulose nanofiber fabricated using two kinds of

grinding method," *Material (Basel)* 15(20), article 7058. DOI: 10.3390/ma15207048

Xu, F., Yang, L., Liu, Z., and Chen, G. (2021). "Numerical investigation on the hydrodynamics of Taylor flow in ultrasonically oscillating microreactors," *Chemical Engineering Science* 235, article 116477. DOI: 10.1016/j.ces.2021.116477

Yi, T., Zhao, H.., Mo, Q. Pan, D., Liu, Y., Huang, L., Xu, H., Hu, B., and Song, H. (2020). "From cellulose to cellulose nanofibrils-a comprehensive review of the preparation and modification of cellulose nanofibrils," *Materials (Basel)* 13(22), article 5062. DOI: 10.3390/ma13225062

Zhang, K., Su, Y., and Xiao, H. (2020). "Preparation and characterization of nanofibrillated cellulose from waste sugarcane bagasse by mechanical force," *BioResources* 15(3), 6636-6647. DOI: 10.15376/biores.15.3.6636-6647

Article submitted: August 23, 2024; Peer review completed: Sept. 15, 2024; Revised version received and accepted: November 5, 2024; Published: November 15, 2024.
DOI: 10.15376/biores.20.1.438-451